A Spatial Cognition Model Integrating Grid Cells and Place Cells

Gonzalo Tejera
Facultad de Ingeniería
Universidad de la República
Montevideo, Uruguay
gtejera@fing.edu.uy

Martin Llofriu
Computer Science and Engineering
University of South Florida
Tampa, FL, USA
mllofriualon@mail.usf.edu

Alejandra Barrera
Departamento de Computación
Instituto Tecnológico Autónomo de Mexico
Mexico City, Mexico
abarrera@itam.mx

Alfredo Weitzenfeld
Computer Science and Engineering
University of South Florida
Tampa, FL, USA
aweitzenfeld@usf.edu

***Abstract*—Grid cells and place cells have shown to play an important role in spatial cognition in rats. While place cells provide global localization from external environment information, grid cells provide a "neural odometry" for path integration from internal vestibular information. In this paper we describe a spatial cognition model integrating grid cells and place cells from behavioral and neurophysiological brain studies in rats. Grid cell firing is generated from a linear oscillatory interference model that includes a reset mechanism to overcome errors in "neural odometry" readings. The model is evaluated in simulation. Future work is discussed including extensions to the model and evaluation under physical robots.**

Keywords— spatial cognition, hippocampus, entorhinal cortex, place cells, grid cells

I. Introduction

We present in this paper a model for spatial cognition integrating grid cells and place cells from behavioral and neurophysiological brain studies in rats. The model is composed primarily of grid cells in the Medial Entorhinal Cortex (MEC) and place cells in the Hippocampus used to generate "neural odometry" and spatial localization in rats. The current work describes spatial cognition exploiting distal cues for localization and "neural odometry" for path integration. The concept of a cognitive map in the brain was first proposed by Tolman [3] as the essential module responsible for estimating the rat's position in the environment. O'Keefe and Nadel located the cognitive map within the brain's hippocampus [4]. The cognitive map is learned from the acquisition of external information from the environment [5], and is used by rats and other animals for path integration [6]. The discovery of place cells in the rat's hippocampus was first published by O'Keefe and Dostrovsky [7]. These neurons were considered the main component of the cognitive map and were termed place cells due to the high correlation between their firing and the rat location in the environment [8]. Studies have related the response of place cells to both kinesthetic, i.e. idiothetic cues, and distal, i.e. allothetic, cues [9]. The discovery of grid cells in the rat's Medial Entorhinal Cortex (MEC) was first published by Fyhn et al [10]. They suggested that grid cell firing signaled the rat's changing position representing a "neural odometry" for navigation. Hafting et al [11] showed that grids assume similar phases and orientations with respect to external landmarks on repeated exposures to the same environment independent of initial starting location. McNaughton et al [12] concluded that in a sufficiently large experimental environment, MEC cells could exhibit a grid-like structure of firing fields repeating at regular intervals that is independent of the size and shape of the environment. Grid cells are considered to be key in ensuring stable spatial representation during rat navigation [13]. Additionally, grid cells have been shown to integrate relative information from head direction cells [14]. Grid cells are thought to be the core of the path integration system [15].

There is an extensive bibliography of spatial cognition models inspired on place cells in the rat's hippocampus, and some that include path integration [16, 17], with direct correlation of distal cues to rat position [8], or their combination [9]. Examples of spatial cognition models include Burgess, Recce, and O'Keefe [18], Brown and Sharp [19], Redish and Touretzky [20], Guazzelli, Corbacho, Bota, and Arbib [21], Gaussier, Revel, Banquet, and Babeau [22], Filliat and Meyer [23], Arleo, Smeraldi, and Gerstner [24], Milford and Wyeth [25, 26], Barrera and Weitzenfeld [27], Dollé, Sheynikhovich, Girard, Chavarriaga, and Guillot [28], Alvernhe, Sargolini, and Poucet [29], and Caluwaerts, Staffa, N'Guyen, Grand, Dollé, Favre-Felix, Girard, and Khamassi [30]. The current paper is novel in its close integration of grid cells and place cells into a spatial cognition model that supports navigation in simulated and real robots. The present model extends prior work described in Barrera, Caceres, Weitzenfeld, and Ramirez-Amaya [31], Barrera, Tejera, Llofriu and Weitzenfeld [32], and Tejera, Barrera, Llofriu and Weitzenfeld [33] by incorporating a newly developed grid cell module based on a linear oscillatory interference model. The current paper presents results from simulations showing the effect of a reset mechanism applied to the path integration module containing the grid cells while a simulated rat navigates in a circular arena during habituation.

The paper is organized as follows: Section II describes our spatial cognition model integrating grid cells and place cells; Section III describes the grid cells module, Section IV describes the place cells module; Section V presents simulation

results on the different modules and complete system; and Section VI provides conclusions and discussion of future work.

II. Spatial Cognition Model

The current work has been developed as an extension to the Barrera-Weitzenfeld model [27]. The main components of the model are shown schematically in Figure 1. The current paper focuses on the Kinesthetic and Path Integration modules that feed the Place Representation as shown in Figure 2.

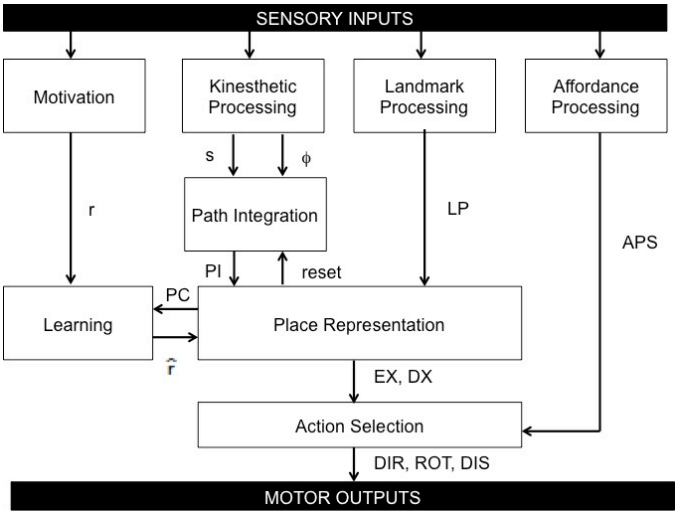

Fig. 1. The spatial cognition model extended from Barrera-Weitzenfeld [27] consisting of the following modules: (1) Kinesthetic Processing (KP) updating the velocity of the rat as it navigates an arena, (2) Path Integration (PI) incorporating grid cells, (3) Landmark Processing (LP) processing landmark-related spatial positioning, (4) Affordance Processing (AF) inspired in Gibson's work [34, 35] discriminating among different possible orientations for navigation, (5) Motivation computing the rat's hunger drive and producing a basic set of reward signals that are transmitted to the learning module, (6) Place Representation (PC) representing the space as an integration of grid cells with landmark information, and containing place cells and the world graph layer, (7) Learning module implemented using Q-Learning [31], and (8) Action Selection generating the resulting rat motions as output to the model.

The spatial cognition model consists of the following modules:

(1) Kinesthetic Processing (KP) represents vestibular motion information from the body of the rat, specifically speed and angular rotation,

(2) Path Integration (PI) represents grid cell firing patterns that take into consideration kinesthetic information from the rat,

(3) Landmark Processing (LP) represents distal cues or landmark-related spatial positioning and orientation,

(4) Affordance Processing (AF), inspired in Gibson's work [34, 35], represents discrimination among different possible orientations for navigation,

(5) Motivation represents the rat's hunger drive and produces a basic set of reward signals that are transmitted to the Learning module,

(6) Place Representation (PC) contains the Place Cell Layer (PCL) and the World Graph Layer (WGL) [27, 31, 32]. The World Graph Layer produces a topological map representing locations in space linking information related to: Path Integration, Landmark Processing, Place Cells and rewards from Learning. Hebbian learning [36] is used for connectivity among layers in the modules.

(7) Learning module represents the reinforcement learning component of the model. This module was originally implemented as an Actor-Critic architecture [27, 37], and it is currently implemented using Q-learning [31].

(8) Action Selection represents the output of the model in terms of rat motions.

Figure 2 describes in more detail the Kinesthetic Processing and Path Integration modules that are the main components being described in the present work. The Kinesthetic Processing modules provide vestibular information from the rat, in particular linear velocity s, angular velocity ω, and head direction information ϕ obtained from the head direction cells. The Path Integration module is based on a linear oscillatory interference model [38, 39], combining output from multiple Band Cells [38, 40, 41] to generate Grid Cells firing. This firing represents the output to the Path Integration (PI) module.

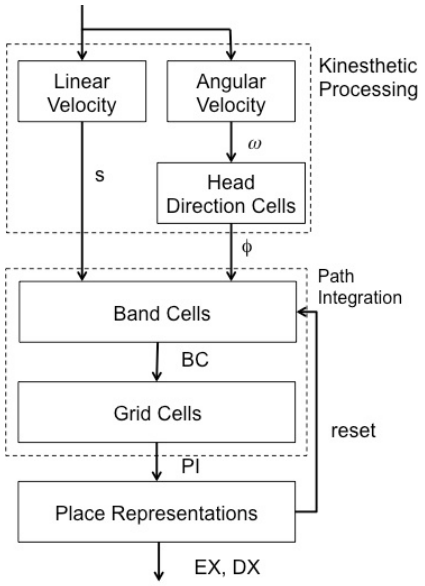

Fig. 2. Kinesthetic Processing and Path Integration modules consisting of vestibular motion information in the Kinesthetic Processing module, and Band Cell and Grid Cell layers in the Path Integration module. A reset mechanism is included in the Band Cell oscillations to keep them in phase.

III. Grid Cells

The Path Integration module is based on a linear oscillatory interference model, as proposed by Burgess et al [38] and Hasselmo et al [39], to generate grid cell firing. This model computes subthreshold membrane potential oscillations corresponding to rhythmic fluctuations of voltage difference in the neurons. Figure 3 provides an illustration of how three band cells with head direction orientations varying in 120° combine to generate a single grid cell that fires in a triangular configuration.

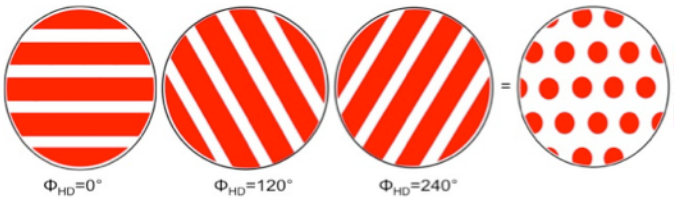

Fig. 3. Grid Cell field formation from Band Cells combining at 3 different Head Direction Cell orientations varying in 120° [38][39].

Figure 4 provides an illustration of how grid cell firing patterns are generated at different positions in the MEC. Variations in dorsal and ventral firing fields in entorhinal cortex produce corresponding firing field dorso-ventral organization in place cell as proposed by Burgess et al [38].

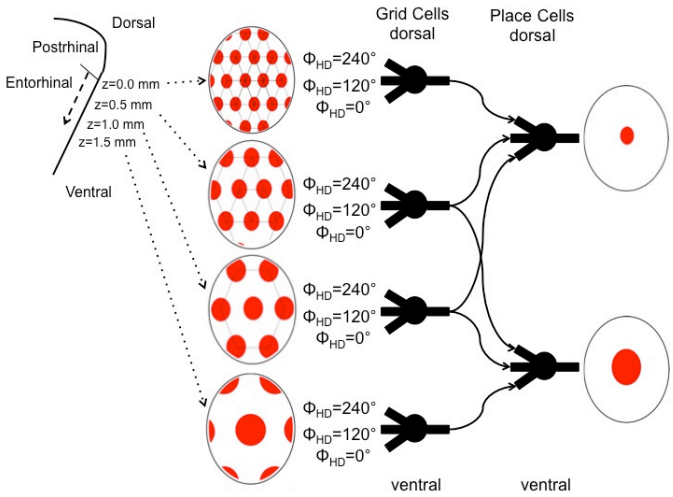

Fig. 4. Proposed grid cell to place cell interconnectivity [42]. Place cells receive input from grid cells with similar spatial phase but having a diversity of spacings and orientations. Grid cell subthreshold firing taken from [39], where neurons show higher frequency of subthreshold oscillations in more dorsal entorhinal cortex and lower frequency in ventral slices, as distance in z-axis increases from the dorsal border with postrhinal cortex producing firing with larger spacing in the grid cells and correspondingly in the place cells.

The spacing of the grid cells firing pattern increases along the dorsal to ventral axis of the entorhinal cortex (*z*-axis), resulting in smaller grid cell fields for neurons in the most dorsal portion of entorhinal cortex (near the border with the postrhinal cortex) and larger firing fields in the more ventral regions of the entorhinal cortex [11]. Based on experimental data obtained from the postrhinal border [39], the change in subthreshold oscillation frequency *f* (in Hz) is equivalent to the inverse of the period *T* (in sec) of subthreshold oscillations relative to distance from postrhinal border (z, in mm), as described by (1-3) and illustrated in Figure 4.

$$T(z) = 0.094\,z + 0.13 \tag{1}$$

$$f(z) = 1/T(z) \tag{2}$$

$$f(z) = 1/(0.094\,z + 0.13) \tag{3}$$

Based on the experimental data [39], grid cell field spacing G (in cm) relative to dorsal–ventral position z (in mm) results in a linear relationship. Thus, the grid cell spacing function $G(z)$ and the subthreshold oscillation period function $1/f(z)$ can be scaled to one another by an experimentally determined function $H(z)$, that is assumed to be a constant H, as described in (4).

$$G(z) = H/f(z) \tag{4}$$

In the range of the experimental data, the value of this experimentally determined constant is approximately 300 Hz-cm. The H constant can be used to estimate the spacing G for a given subthreshold oscillation frequency f, as shown in (5).

$$G(z) = 300/f(z) \tag{5}$$

Table I shows approximate period, frequency and spacing value examples for a given z value based on (1-5).

TABLE I. GRID CELLS FIELD SPACING

z (mm)	Grid Cell Firing		
	T(z) (sec)	*f(z) (Hz)*	*G(z) (cm)*
0.0	0.13	7.69	39
0.5	0.177	5.65	53
1.0	0.224	4.46	67
1.5	0.271	3.69	81

According to Hasselmo et al [39], the linear fit to the membrane potential oscillation (mpo) period has a slope of about 0.1 Hz per mm of distance from postrhinal border. Multiplication by the scaling factor 300 gives a slope of 30 cm of grid spacing per mm of distance from the postrhinal border for the linear fit to the grid cell spacing G.

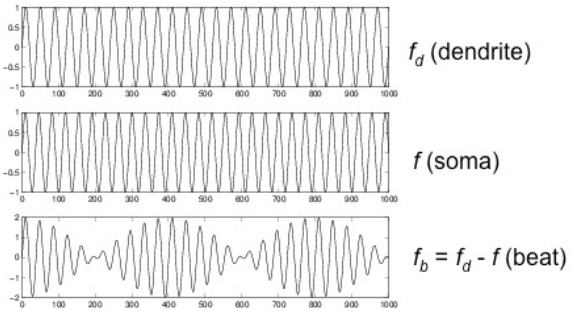

Fig. 5. The beat frequency f_b is computed by the difference in soma oscillation frequency f and dendrite oscillation frequency f_d.

We present in equations (6-18) the linear oscillatory interference model as described by Hasselmo et al. [39]. The membrane voltage oscillation (mpo) of the neuron is defined by $V(t)$ as the sum of soma oscillations at frequency f and dendritic oscillations at frequency f_d as described by (6). *BC* from Figure 2 corresponds to a layer of band cells with oscillations defined by $V(t)$ in (6).

$$V(t) = \cos(f 2\pi t) + \cos(f_d 2\pi t) \tag{6}$$

The dendrite oscillation frequency f_d is given by adding the soma oscillation frequency f and the beat oscillation frequency f_b as described in (7), and illustrated in Figure 5.

$$f_d = f + f_b \tag{7}$$

The rat velocity v can be obtained from rat speed s and head direction ϕ relative to the preferred head direction ϕ_{HD} as given by (8).

$$v = s\cos(\phi - \phi_{HD}) \tag{8}$$

The distance between firing locations is determined from the beat oscillation spatial wavelength λ_b, and can be computed from the rat velocity v and beat period T_b, as shown by (9), where T_b is the inverse of the beat frequency f_b.

$$\lambda_b = vT_b = v/f_b = s\cos(\phi - \phi_{HD})/f_b \tag{9}$$

In order to keep the spatial firing stable, the spatial wavelength λ_b should remain constant, and independent of changes in speed s and heading direction ϕ. This can be achieved by defining the beat frequency f_b relative to changes in speed s and angle of movement, as shown by (10).

$$f_b = Bs\cos(\phi - \phi_{HD}) \tag{10}$$

The constant B introduced in (10) is equivalent to the inverse of the spatial wavelength λ_b, as shown in (11).

$$B = 1/\lambda_b \tag{11}$$

The dendrite oscillation frequency f_d is redefined by combining (7) and (10), as shown in (12).

$$f_d = f + Bs\cos(\phi - \phi_{HD}) \tag{12}$$

Equation (12) results in a constant spatial wavelength in the dimension of one head direction cell, corresponding to the output of one band cell, as proposed by Burgess et al [38] and Hasselmo et al [39].

Additionally, Hasselmo et al [39] applied trigonometry to compute the relationship between grid cell firing space G and beat spatial wavelength λ_b, and constant B defined from (11), as shown in (13).

$$G = \lambda_b(2/\sqrt{3}) = 2/\sqrt{3}\mathrm{B} \tag{13}$$

A new constant B_H is introduced by Hasselmo et al [39], using the experimental constant H from (4) and (5), as shown in (14).

$$B_H = 2/\sqrt{3}H = 0.00385 \tag{14}$$

From (4) and (14), $G(z)$ can be defined as shown in (15).

$$G(z) = 2/(\sqrt{3}B_H f(z)) \tag{15}$$

Combining (14) and (15), B is redefined as shown in (16).

$$B = B_H f(z) \tag{16}$$

Finally, the dendrite frequency f_d given in (12) may be rewritten as shown in (17).

$$f_d = f + fB_H s\cos(\phi - \phi_{HD}) \tag{17}$$

Grid cell firing $g(t)$ is generated by combining three band cells, each corresponding to $V(t)$, as shown in (18).

$$g(t) = \Theta\left[\prod_{HD}(\cos(f2\pi t) + \cos\left(\left(f + fB_H s\cos(\phi - \phi_{HD})\right)2\pi t\right) + \varphi\right] \tag{18}$$

In (18), Θ is a step function, and Π represents the product across soma and the dendrites receiving input from the three different head direction cells with selectivity angles at $\phi_{HD} = 0$, $\phi_{HD} = 120$, $\phi_{HD} = 240$. f represents the threshold oscillation frequency and constant B_H represents grid cell field spacing, where both are experimentally determined. The variable φ represents the initial phase (described as a vector of phase shifts) of each membrane potential oscillation in the neuron.

IV. Place Cells

The Place Representation module in Figure 1 receives input from the Path Integration (PI) module containing the Grid Cells and the Landmark Processing (LP) module containing an egocentric representation of distal cues from local visual perception. In order to generate each Place Cell layer neuron j (PC_j), the outputs of these modules are multiplied by corresponding connection weights w (updated using Hebbian learning rules [36]) as shown by (19).

$$PC_j = \sum_i PI_i\, w_{ij}^{pi} + \sum_i LP_i\, w_{ij}^{lp} \tag{19}$$

The detailed description of the Place Representation module is presented in Barrera and Weitzenfeld [27]. In addition to Place Cells, the Place Representation module also contains the World Graph Layer (WGL), producing a topological map of the environment. As the rat moves, the system searches for the best match between the current activation pattern produced by the Place Cells (PC) and all Patterns (PAT) previously stored in WGL to localize the rat in the environment. If a matching pattern ($pat \in$ PAT) is found, the rat is located at the corresponding WGL node representing a spatial location [27]. This search process involves the computation of the similarity degree (SD) as an Euclidean distance between the current activation pattern PC and a stored pattern $pat \in$ PAT as shown in (20).

$$SD(pat, PC) = \sqrt{\sum_{i=1}^{N_{PC}} (pat_i - PC_i)^2} \tag{20}$$

N_{pc} is the PC layer dimension, and pat corresponds to a pattern stored in a WGL node having same dimension as the PC layer. The stored pattern pat from all WGL nodes with closest similarity to PC is obtained by computing the minimum value for all SD functions as described in (21).

$$pat: min_{pat \in PAT}\, SD(pat, PC) \quad (21)$$

If a *pat* is found in (21), with an SD value below a threshold set to 90, then the rat is considered to be located at the corresponding WGL node; otherwise a new node is created in WGL (see [27] for more detail on this process).

Finding a valid *pat* in (21) also results in the generation of a *reset* signal to the band cells shown in Figure 2. The *reset* signal is important as it adjusts grid cells firing to the correct location in order to overcome noise from incorrect readings of speed *s* in (17). The reset signal results in an adjustment of the dendritic phase of $V(t)$ in (6) and g(t) in (17).

In (22) we define the soma component $x_s(t)$ from inside the cosine function in (6) and (17). In (23) we define the dendritic component $x_d(t)$ from inside the cosine function in (6) and (17). In (24) we create a new dendritic component $x'_d(t)$ providing the reset mechanism that enables the dendritic oscillation $x_d(t)$ to move closer to the soma oscillation $x_s(t)$.

$$x_s(t) = f 2\pi t \quad (22)$$

$$x_d(t) = f_d 2\pi t \quad (23)$$

$$x'_d(t) = x_d(t) + \gamma\,(x_s(n) - x_d(t)) \quad (24)$$

The γ parameter is set heuristically to 0.8. Note that if the value of γ is 0, then no update would be made to the dendritic oscillation $x_d(t)$, while a value of 1 will make the $x_d(t)$ oscillation equal to the soma oscillation $x_s(t)$.

V. Simulation Results

In this section we describe simulation results for Grid Cells and Place Cells, and an evaluation of the reset mechanism for loop closure during rat spatial navigation.

A. Grid Cells

Figure 6 (left) shows a rat navigation trajectory in an open arena obtained from recordings by Hafting et al [11]. Figure 6 (right) shows the corresponding grid cell firing for a single neuron (17), forming a periodic triangular grid covering the complete environment.

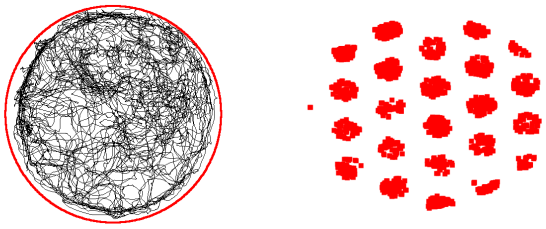

Fig. 6. The following simulation corresponds to: (a) open field arena showing in black the rat trajectory navigation as registered by Hafting et al [11], and (b) in red the firing of a single MEC grid cell for the corresponding simulated trajectory navigation where each red dot marks the location of the rat when a single spike was emitted by the single grid cell.

Figure 7 shows grid cell firing spacing under various z values from Figure 4.

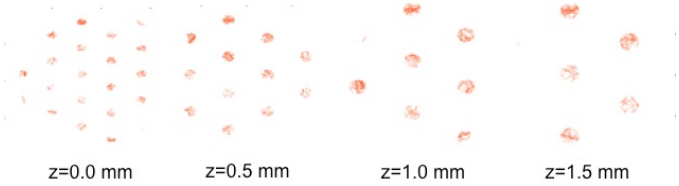

Fig. 7. Firing fields of four different grid cells recorded simultaneously while a rat ran around in a circular arena, where z corresponds to spacing registered at postrhinal border: z=0.0mm, z=0.5mm, z=1.0mm and z=1.5mm.

Figure 8 shows grid fields for different spatial orientation values of ϕ_{HD}.

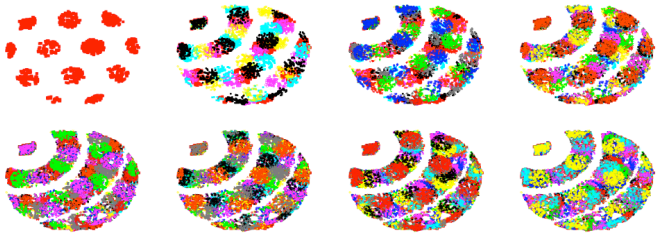

Fig. 8. Firing fields of grid cells with different ϕ_{HD} spatial orientations but similar phase and spacings starting at ϕ_{HD} = -30° (yellow), up to 15° (purple), with increments of 15°. Each figure shows an increasing number of grid cells 1, 5, 10, 15, 20, 25, 30, and 35, correspondingly.

Figure 9 shows peak firing for grid cells for different spatial phase values φ.

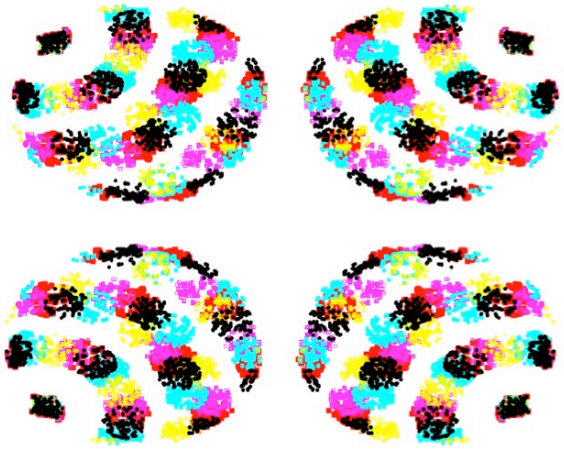

Fig. 9. Firing fields of grid cells with different initital φ spatial phases with similar spacing and orientation, where φ is varied in 90° increments.

The arena in Figure 6 is mapped with a regular grid of 69 vertices to balance computational efficiency versus field coverage, where 10 different grid cells fire concurrently at any given vertex. Thus, a total of 690 grid cells are uniformly distributed in the circular environment.

B. Place Cells

The Place Cells (PC) are generated in (19) by combining input from the Path Integration (PI) module and the Landmark

Processing (LP) module. PC patterns are used to generate activation patterns at each location in the World Graph Layer (WGL). Figure 10 illustrates this process, where a robot in a circular arena is shown in "Global Image". The robot camera perceives a "Panoramic Image" of the arena composed of multiple "Local Views". The pre-established distal cues or landmarks are processed by color by the "Landmark Perceptual Schema" to produce different LPS with varying distance and orientation. Figure 10 shows a sample output of the graphical interface consisting of a Local View, Panoramic Image, Global Image, Landmarks Perceptual Schema, Action Selection Schema, and World Graph Layer.

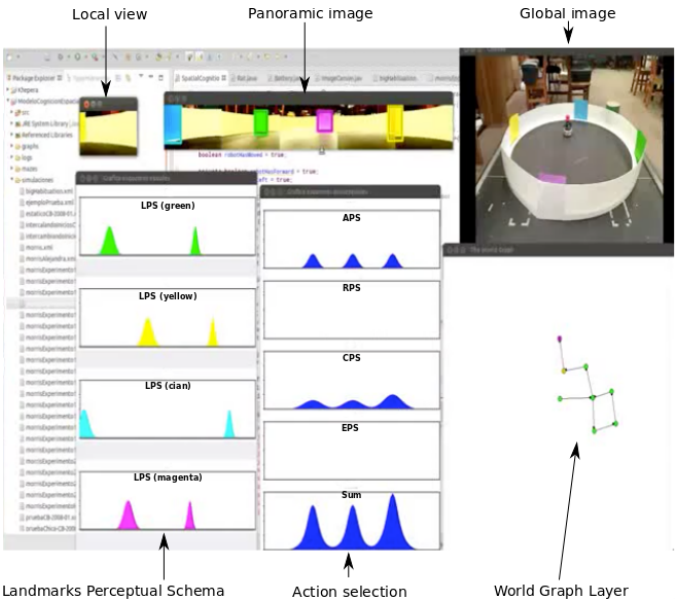

Fig. 10. The figure shows a Morris-like circular arena in the top right "Global Image". The other images in the top correspond to the "Panoramic Image" composed of multiple "Local Views" as pereceived by the robot local camera. The pre-established distal cues or landmarks are processed by color by the "Landmark Perceptual Schema" to produce different LPS activations combining distance and orientation for each colored landmark, in this case 4: green, yellow, cyan and magenta. The graph to the right of the various LPS is the "Action Selection" representing the motion output from the model. This graph produces a "Sum" of "Affordance Perceptual Schema" (APS), "Random Perceptual Schema" (RPS), "Curiosity Perceptual Schema" (CPS), and "Expectation Perceptual Schema" (EPS) or "Expectation of Maximum Reward" (EMR). Finally, the bottom right corresponds to the World Graph Layer (WGL) nodes showing the current location of the robot (in magenta) and its previous location (in yellow). Green nodes represent previously visited locations.

The robot experiments shown in Figure 10 are based on circular arenas inspired by Morris' water mazes [1][2]. In these experiments, having water when using real rats, the animal needs to locate a hidden platform at a fixed location inside the water maze. In Figure 10, the arena is a dry version of Morris' water maze and the hidden platform would correspond to a mark on the floor of the arena that can only be seen when the robot is on top of it. Navigation in the arena requires creation of a cognitive map combining landmark and path integration of visited locations to learn a route to the hidden goal after several trials. In the work presented in the current paper there is no goal, but rather, the robot does a habituation or pre-trial in the environment to generate the corresponding cognitive map prior to use learning for goal-oriented tasks. During this phase EPS has no activity since no rewards are given to the rat. The most important component during habituation is the CPS component corresponding to curiosity based on a motivational factor promoting the exploration of unknown portions of the environment.

C. *Loop Closure during Navigation*

Loop closure evaluates the correct localization of the rat using the spatial cognition model. For this purpose nodes in WGL have to be mapped correctly during multiple navigations. This is also the purpose of rat habituation or the pre-trial stage, as the rat navigates a new arena where no goal is present. Loop closure tests if a rat is able to return to a previously visited location corresponding to an existing node in WGL. Figure 11 shows various examples of WGL maps constructed in relation to the circular arena from Figure 10. In Figure 11 (moving clockwise starting at the top left): (a) WGL map with no loop closure errors where all nodes are correctly connect to their 8 neighbors (note that in Figure 10, node creation was done using 4 neighbors only); (b) WGL map with 5 loop closure errors corresponding to new nodes assigned to already mapped space; (c) WGL map with 250 loop closure errors; and (d) WGL map with 500 loop closure errors. As can be appreciated from this graph, as the number of loop closure errors increase, this results in incorrect localization where distant locations may be perceived as next to each other.

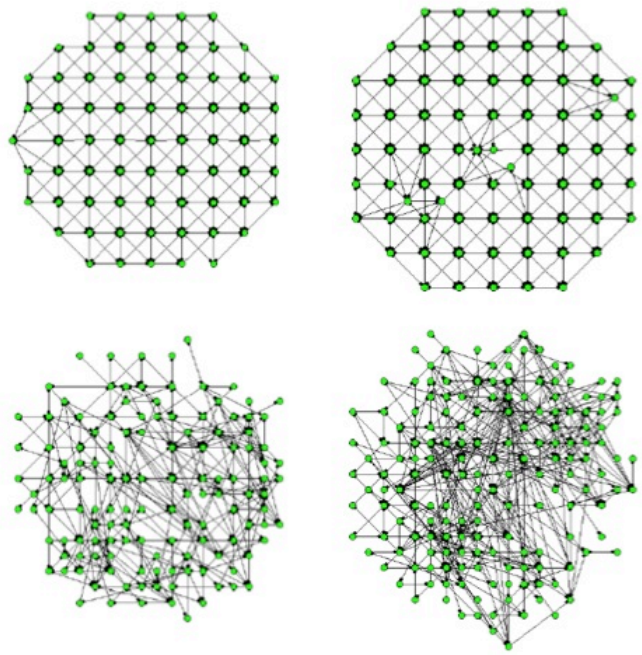

Fig. 11. WGL map corresponding to the circular arena in Fig 10. Moving clockwise from top left: (a) no loop closure errors, (b) 5 loop closure errors, (c) 250 loop closure errors, and (d) 500 loop closure errors.

The loop closure problem can be further analyzed by simulating inaccuracies in the correct velocity being read. This analysis provides further insight into the robustness of the linear oscillatory interference model presented in this paper as part of the spatial cognition model. For these new tests, noise is added to the linear velocity s as shown in Figure 12. A noisy

velocity *s'* is introduced, as described by (25), and applied to the generation of grid cells firing computed in (17).

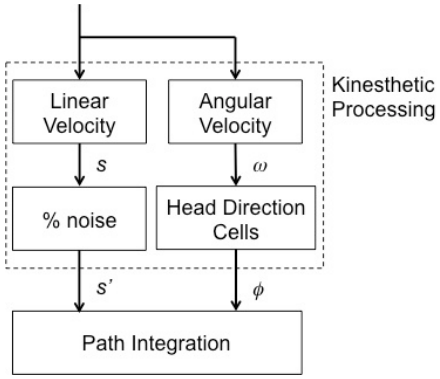

Fig. 12. Introduction of noise into the model by modifying linear velocity read be the kinesthetic processing module.

$$s' = s(1 + \xi * factor) \quad (25)$$

In (25), ξ is a random variable with normal distribution, having parameters μ_{err_num} and $\sigma^2_{err\_num}$. The *factor* parameter is set in the range of 0-5, and is used to increase the level of noise. Table II provides an average error comparison during loop closure in WGL. The table contrasts different values in (25), having a noise factor *N* that varies from 1-5: DRL*N* (Dynamic Remapping Layer) corresponds to the model by Barrera and Weitzenfeld [27], G*N* corresponds to the current model with grid cells but no reset, and G&R*N* corresponding to the current model with grid cells and reset. The table contrasts loop closure error values: *min*, *mean*, *variance* and *max*.

TABLE II. AVERAGE ERROR COMPARISON DURING LOOP CLOSURE

factor	=0	=1	=1	=4	=4	=5	=5
PI	DRL	DRL	G1	G4	G&R4	G5	G&R5
min	39	503	0	24	0	57	30
mean	87	570	0.57	123	23	174	75
variance	25	26	1.33	33	15	66	21
max	133	621	4	187	51	373	105

Figure 13 shows the number of loop closure errors in relation to actions taken by the robot during simulation, where actions correspond to motion steps. It is important to note that the original DRL module resulted in the largest number of loop closure errors, while the introduction of Grid Cells with reset into the Path Integration module resulted in lowest number of loop closure errors. More specifically, G&R*N* for *N*<4, did not generate any loop closure errors.

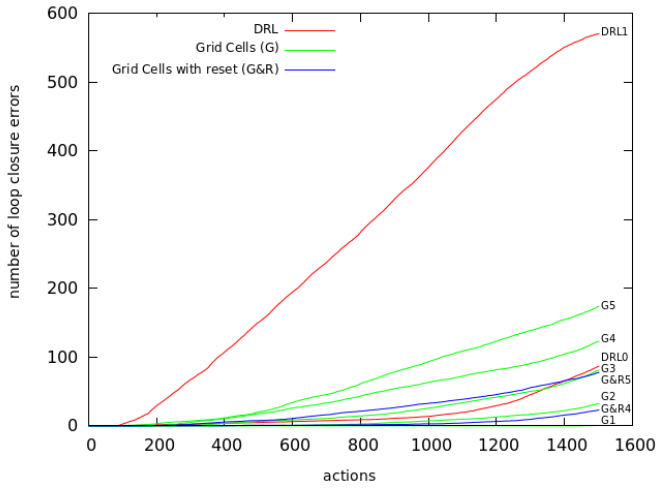

Fig. 13. Average error comparison during loop closure where *N* varies from 1-5: DRL*N* (Dynamic Remapping Layer) from the model by Barrera and Weitzenfeld [27], G*N* corresponding to the current model with grid cells but no reset, and G&R*N* corresponding to the current model with grid cells and reset.

VI. CONCLUSIONS AND DISCUSSION

The goal of this paper has been to evaluate a spatial cognition model integrating grid cells and place cells. The current work extends the original model by Barrera-Weitzenfeld [27][31][32] by incorporation of the Grid-Cell based Path Integration module representing "neural odometry". In particular, the current paper extends the analysis and preliminary results obtained in [33]. The Grid Cell layer is based on a linear oscillatory interference model [38, 39]. Noise in velocity reading is introduced into the model to evaluate loop closure errors during robot navigation. The neural model was developed using the Neural Simulation Language [43] as it allows incremental incorporation of neurophysiological details as they become available. The system interacts via wireless communication with the robot to process visual input and issue motion commands. As part of future work we plan to compare the results obtained from the linear oscillatory interference model to those produce by an attractor model [44, 45]. Additionally, we are planning to perform full goal-oriented navigation experiments while contrasting the effect of varying spacing in grid cell firing.

ACKNOWLEDGMENT

This work is funded by NSF IIS Robust Intelligence research collaboration grant #1117303 at USF and U. Arizona entitled "Investigations of the Role of Dorsal versus Ventral Place and Grid Cells during Multi-Scale Spatial Navigation in Rats and Robots," and supported in part by the "Agencia Nacional de Investigacion e Innovación (ANII)" and by the "Asociación Mexicana de Cultura, A. C."

REFERENCES

[1] Morris, R. G. M., Spatial localization does not require the presence of local cues. Learning and Motivation 12: 239 –260 (1981).

[2] Morris, R. G. M., Developments of a water-maze procedure for studying spatial learning in the rat, Journal of Neuroscience Methods, Elsevier, vol 11, pp. 47-60 (1984).

[3] Tolman, E., “Cognitive maps in rats and men,” Psychological Review 55: 189-208 (1948).

[4] O’Keefe, J. and Nadel, L., “The hippocampus as a cognitive map,” Oxford University Press (1978).

[5] Poucet, B., “Spatial cognitive maps in animals: new hypotheses on their structure and neural mechanisms”, Psychological Review 100 (2): 163–182 (1993).

[6] Etienne, A. S. and Jeffery, K. J., “Path integration in mammals. Hippocampus,” 14 (2): 180–192 (2004).

[7] O’Keefe, J., and Dostrovsky, J., “The hippocampus as a spatial map: preliminary evidence from unit activity in the freely moving rat,” Brain Research, 34(1): 171 – 175 (1971).

[8] McNaughton B. L., Knierim J. J., and Wilson, M. A. “Vector encoding and the vestibular foundations of spatial cognition”. In Gazzaniga, M. (Ed.), The cognitive neurosciences, MIT Press, Boston, pp. 585-595 (1994).

[9] Jeffery, K. J., and O’Keefe, J. M., Learned interaction of visual and idiothetic cues in the control of place field orientation. Experimental Brain Research – 127: 151-161 (1999).

[10] Fyhn, M., Molden, S., Witter, M., Moser, E. and Moser, MB., Spatial Representation in the Entorhinal Cortex, Science, Vol 305, pp 1258-1264, Sept (2004).

[11] Hafting, T., Fyhn, M., Molden, S., Moser, MB., and Moser, E., Microstructure of a spatial map in the entorhinal cortex, Nature, Vol 436, pp 801-806, Aug (2005).

[12] McNaughton, B., Battaglia, F, Jensen, O., Moser, E., and Moser, M.B., Path integration and the neural basis of the ‘cognitive map’, Nature Reviews, Neuroscience, Vol 7, pp 663-678, Aug (2006).

[13] Moser, E., Kropff, E., Moser, MB., Place Cells, Grid Cells, and the Brain’s Spatial Representation System, Annual Reviews in Neuroscience, Vol 31, pp 69-89 (2008).

[14] Taube J.S., Head direction cells and the neurophysiological basis for a sense of direction. Prog. Neurobiol. 55:225–56 (1998).

[15] Navratilova, Z., Giocomo, LM., Fellous, JM., Hasselmo, M., and McNaughton B., Phase Precession and Variable Spatial Scaling in a Periodic Attractor Map Model of Medial Entorhinal Grid Cells with Realistic After-Spike Dynamics, Hippocampus (2011).

[16] Mittelstaedt, M., Mittelstaedt, H. “Homing by path integration in a mammal,” in Avian Navigation, Papi, F., Wallraff, H. G., Springer Verlag, Berlin, pp. 290-297 (1982).

[17] Etienne, A. S. and Jeffery, K. J. “Path integration in mammals”. Hippocampus 14 (2):180–192 (2004).

[18] Burgess, N., Recce, M., and O’Keefe, J.“A model of hippocampal function”. Neural Networks 7 (6-7): 1065-1081 (1994).

[19] Brown, M. A., Sharp, P. E. “Simulation of Spatial Learning in the Morris Water Maze by a Neural Network Model of the Hippocampal Formation and Nucleus Accumbens”, Hippocampus 5: 171-188 (1995).

[20] Redish, A. and Touretzky, D. “Cognitive maps beyond the hippocampus”. Hippocampus 7 (1): 15-35 (1997).

[21] Guazzelli, A., Corbacho, F. J., Bota, M. and Arbib, M. A. “Affordances, motivation, and the world graph theory”. Adaptive Behavior 6 (3-4): 435--471 (1998).

[22] Gaussier, P., Revel, A., Banquet, J. P., Babeau, V. “From view cells and place cells to cognitive map learning: processing stages of the hippocampal system,” Biological Cybernetics 86, pp. 15-28 (2002).

[23] Filliat, D., Meyer, J.-A. . “Global Localization and Topological Map Learning for Robot Navigation,” in From Animals to Animats 7 Proceedings of the Seventh International Conference on Simulation of Adaptive Behavior, edited by Hallam et al., The MIT Press, pp 131-140 (2002).

[24] Arleo, A., Smeraldi, F., and Gerstner, W. “Cognitive navigation based on nonuniform Gabor space sampling, unsupervised growing networks, and reinforcement learning”. IEEE Transactions on Neural Networks 15 (3): 639-652 (2004).

[25] Milford, M., Wyeth, G. “Spatial mapping and map exploitation: a bio-inspired engineering perspective”. In Winter, S., Duckham, M., Kulik, L. and Kuipers, B. (Eds.), Spatial Information Theory (pp. 203-221), Heidelberg, Germany, Springer-Verlag (2007).

[26] Milford, M., Wyeth, G. “Persistent navigation and mapping using a biologically inspired SLAM system”. The International Journal of Robotics Research 29(9): 1131-1153 (2010).

[27] Barrera, A., and Weitzenfeld, A. Biologically-inspired Robot Spatial Cognition based on Rat Neurophysiological Studies, Journal of Autonomous Robots, Springer, Vol. 25, No. 1-2, pp. 147-169 (2008).

[28] Dollé, L., Sheynikhovich, D., Girard, B., Chavarriaga, R., and Guillot, A. “Path planning versus cue responding: a bioinspired model of switching between navigation strategies”. Biological Cybernetics, 103(4):299-317 (2010).

[29] Alvernhe, A., Sargolini, F., Poucet, B. . “Rats build and update topological representations through exploration”. Animal Cognition, 15: 359–368 (2011).

[30] Caluwaerts K, Staffa M, N'Guyen S, Grand C, Dollé L, Favre-Felix A, Girard B, and Khamassi M , “A biologically inspired meta-control navigation system for the Psikharpax rat robot”, Bioinspiration&Biomimetics, Vol. 7, No. 2, DOI 10.1088/1748-3182/7/2/025009 (2012).

[31] Barrera, A., Caceres, A., Weitzenfeld, A., and Ramirez-Amaya, V., Comparative Experimental Studies on Spatial Memory and Learning in Rats and Robots, Journal of Intelligent and Robotic Systems, Volume 63, Numbers 3-4,361-397, Sept (2011).

[32] Barrera, A., Tejera, G., Llofriu, M., & Weitzenfeld, A., “Learning Spatial Localization: From Rat Studies to Computational Models of the Hippocampus”, Spatial Cognition & Computation, Vol. 15, No. 1, pp. 27-59 (2015).

[33] Tejera, G., Barrera, A., Llofriu, M., Weitzenfeld, A., “Solving uncertainty during robot navigation by integrating grid cell and place cell firing based on rat spatial cognition studies”, Proc. ICAR 2013, Nov (2013).

[34] Gibson, J. J., The visual perception of objective motion and subjective movement. Psychological Review, 61, 304-314 (1954).

[35] Gibson, J. J., The theory of affordances. In R. Shaw & J. Bransford (Eds.), Perceiving, acting, and knowing:Toward an ecological psychology (pp. 67-82). Hillsdale, NJ: Erlbaum (1977).

[36] Hebb, D. O., The organization of behavior: a neuropsychological theory. Wiley-Interscience, New York (1949).

[37] Barto, A. G., Adaptive critics and the basal ganglia. In Houk, C., Davis, J. L., Beiser, D. (Eds.), Models ofinformation processing in the basal ganglia, MIT Press, Cambridge, MA, pp. 215-232 (1995).

[38] Burgess N., Barry C., and O’Keefe J., An Oscillatory Interference Model of Grid Cell Firing, Hippocampus 17, 801-812 (2007).

[39] Hasselmo, M., Giocomo, M., and Zilli, E., Grid Cell Firing May Arise From Interference of Theta FrequencyMembrane Potential Oscillations in Single Neurons, Hippocampus, 17, 1252–1271 (2007).

[40] Krupic, J., Burgess, N., and O'Keefe, J., "Neural representations of location composed of spatially periodic bands", Science 337, 853–857 (2012).

[41] Mhatre H, Gorchetchnikov A, Grossberg S., Grid cell hexagonal patterns formed by fast self-organized learning within entorhinal cortex. *Hippocampus* 22(2): 320-334 (2012).

[42] Solstad, T., Moser, E.I., and Einevoll, G.T.,From grid cells to place cells: a mathematical model. Hippocampus 16:1026-1031 (2006).

[43] Weitzenfeld, A., Arbib, M., Alexander, A. The Neural Simulation Language, MIT Press (2002).

[44] Fuhs MC, Touretzky DS, A spin glass model of path integration in rat medial entorhinal cortex. J Neurosci 26:4266 – 4276 (2006).

[45] Bush D, Burgess N, A hybrid oscillatory interference / continuous attractor network model of grid cell firing. *J. Neurosci*., 34: 5065-5079 (2014).